THE JOURNAL OF BIOLOGICAL CHEMISTRY VOL. 288, NO. 19, pp. 13620–13630, May 10, 2013

Death Domain-associated Protein DAXX Promotes Ovarian Cancer Development and Chemoresistance*[S]

Received for publication, December 19, 2012, and in revised form, March 25, 2013 Published, JBC Papers in Press, March 28, 2013, DOI 10.1074/jbc.M112.446369

Wei-Wei Pan[‡§], Jian-Jie Zhou[‡], Xiao-Man Liu[‡], Ying Xu[§], Lian-Jun Guo[‡], Chao Yu[‡], Qing-Hua Shi[¶], and Heng-Yu Fan[‡1]

From the [‡]Life Sciences Institute, Zhejiang University, Hangzhou, 310058, the [§]School of Medicine, Jiaxing University, Jiaxing 314001, and the [¶]School of Life Sciences, University of Science and Technology of China, Hefei 230022, China

Background: The role of DAXX in ovarian cancer development and metastasis has not been investigated before now.
Results: Overexpression of DAXX enhanced ovarian cancer cell proliferation, colony formation, and migration, whereas *Daxx* depletion had the opposite effects.
Conclusion: DAXX promotes ovarian cancer cell proliferation and chemoresistance.
Significance: Modulating DAXX may be an effective strategy for preventing the recurrence and chemoresistance of ovarian cancers.

Understanding the genes involved in apoptosis and DNA damage responses may improve therapeutic strategies for ovarian cancer. The death domain-associated protein DAXX can be either a pro-apoptotic or an anti-apoptotic factor, depending on the cell type and context. In this study, we found that DAXX was highly expressed in human ovarian surface epithelial tumors but not in granulosa cell tumors. In cultured ovarian cancer cells, DAXX interacted with promyelocytic leukemia protein (PML) and localized to subnuclear domains (so-called PML nuclear bodies). A role for DAXX in ovarian cancer cell proliferation, metastasis, and radio/chemoresistance was examined. Overexpression of DAXX enhanced multiple ovarian cancer cell lines' proliferation, colony formation, and migration, whereas *Daxx* depletion by RNA interference had the opposite effects. When transplanted into nude mice, ovarian cancer cells that overexpressed DAXX displayed enhanced tumorigenesis capability *in vivo*, whereas *Daxx* depletion inhibited tumor development. Importantly, *Daxx* induced tumorigenic transformation of normal ovarian surface epithelial cells. *Daxx* also protected ovarian cancer cells against x-irradiation- and chemotherapy-induced DNA damage by interacting with PML. Taken together, our results suggest that DAXX is a novel ovarian cancer oncogene that promotes ovarian cancer cell proliferation and chemoresistance in ovarian cancer cells. Thus, modulating DAXX-PML nuclear body activity may be an effective strategy for preventing the recurrence and chemoresistance of ovarian cancers.

Small molecules that cause DNA damage, such as cisplatin, bleomycin (BLM),[2] etoposide (VP-16), and doxorubicin, are first line anticancer agents for human ovarian cancer whose effects result, in part, from apoptosis induction (1). Chemoresistance remains a major hurdle to successful treatment. Recent evidence indicates that the inability of cancer cells to undergo apoptosis is a key determinant of chemotherapy resistance. Dysregulation of pro-apoptotic mediators, such as FAS, caspases, and p53, and anti-apoptotic pathways, such as AKT, X-linked IAP, and FAS-associated death domain-like interleukin-1b-converting enzyme-like inhibitory protein pathways, has been demonstrated in chemoresistant cells (2, 3).

DAXX was initially identified as a pro-apoptotic protein that bound to the death domain of the CD95 death receptor. By activating the c-Jun NH_2-terminal kinase pathway, DAXX was shown to enhance both CD95-mediated and transforming growth factor-β-dependent apoptosis (4). Interestingly, *Daxx* down-regulation by RNA interference was also associated with increased apoptosis (5). Moreover, targeted disruption of the murine *Daxx* gene resulted in embryonic lethality due to extensive global apoptosis, which suggested that DAXX could also have anti-apoptotic effects (6).

Aside from its controversial role in apoptosis, DAXX is a well established transcription regulator. DAXX can interact with several crucial proteins involved in transcriptional silencing, such as histone deacetylases HDAC1 and HDAC2 and DNA methyltransferase DNMT1. DAXX represses the activity of several transcriptional factors, including C/EBPβ, c-Met, Pax3, Ets1, p53, and its family members p73 and p63, glucocorticoid receptor, androgen receptor, and SMAD4 (7–11).

Consistent with its involvement in transcriptional regulation, DAXX is predominantly a nuclear protein. In the nucleus, it primarily localizes to subnuclear structures, so-called PML-oncogenic domains (PODs), by binding to SUMO-modified PML. Promyelocytic leukemia (PML) protein nuclear bodies (NBs) are macromolecular nuclear domains that are found in virtually all mammalian cells (12). PML nuclear bodies (PML-NBs) have been functionally linked to various fundamental cel-

* This work was supported by National Natural Science Foundation of China Grant 81172473, National Basic Research Program of China Grants 2011CB944504 and 2012CB944403, Natural Science Foundation of Zhejiang Province Grants R2100145 and Y2110873, Science and Technology Bureau Project of Jiaxing Grant 2011AY1048-6, and Basic Scientific Research Funding of Zhejiang University Grant 2011QN81001.
[S] This article contains supplemental Fig. 1.
[1] To whom correspondence should be addressed. Tel.: 86-571-88981370; Fax: 86-571-88981337; E-mail: hyfan@zju.edu.cn.
[2] The abbreviations used are: BLM, bleomycin; PML, promyelocytic leukemia; PML-NB, PML nuclear body; POD, PML oncogenic domain; OSE, ovarian surface epithelium; mOSE, mouse ovarian surface epithelium; MTT, 3-(4,5-dimethylthiazol-2-yl)-2,5-diphenyltetrazolium bromide; FAS, TNF receptor superfamily member 6.

lular processes, including transcriptional control, tumor suppression, and apoptosis regulation (13). In support of the important role of PML and its associated NBs in apoptosis regulation, several apoptotic regulators localize to PML-NBs, and cells from PML-deficient mice display severe apoptotic defects (14). However, the possible involvement of DAXX and PML in the proliferation and apoptosis of ovarian cancer cells has not been examined.

Thus, in this study, we used both ovarian cancer cells and normal ovarian surface epithelial (OSE) cells to investigate the involvement of DAXX and PML in proliferation, metastasis, and DNA damage-induced responses. We found that DAXX and PML were highly expressed in human ovarian cancer tissues and that they enhanced tumor growth, cell migration, colony formation, and resistance to DNA damage insults both *in vitro* and *in vivo*. In addition, DAXX overexpression caused the tumorigenic transformation of normal OSE cells and thus acted as an ovarian cancer oncogene. These results suggest that modulating DAXX-PML nuclear body activity may be an effective strategy for preventing the recurrence and chemoresistance of ovarian cancers.

MATERIALS AND METHODS

Reagents and Cell Culture—Human ovarian cell lines ES-2, SK-OV3, OV2008, and A2780 were purchased from the ATCC. The immortalized mouse ovarian surface epithelium (mOSE) was reported previously (15, 16). All cells were cultured in DMEM (Invitrogen) supplemented with 10% fetal bovine serum (FBS; Hyclone) and 1% penicillin/streptomycin solution (Invitrogen) at 37 °C in a humidified 5% CO_2 incubator.

Mice and Xenograft Models—Mice were housed with a 14:10 h, light/dark schedule and provided food and water *ad libitum*. All animal protocols were in accordance with the National Institutes of Health Guide for the Care and Use of Laboratory Animals. To assess proliferation and metastasis, ovarian cancer cells were injected subcutaneously or intraperitoneally into 8-week-old female athymic nude mice. Four weeks later, primary tumor masses were fixed in 4% paraformaldehyde and embedded in paraffin. Sections (5 μm thick) were prepared and stained with hematoxylin and eosin.

Plasmids and RNA Interference—Expression constructs encoding for full-length *Daxx* (pLEGFP-*Daxx* and HA-*Daxx*) were kindly provided by Dr. K. N. Klempnauer (9). Two duplex oligonucleotides encoding for human *Daxx*-specific short hairpin RNAs (shRNA2, 5′-GATCCTCCCCTCCCACACACCTCTCCTTGGGGAGAGGTGTGTGGGAGGGTTTTTG-3′, and shRNA3, 5′-TCGACAAAAAGGAGTTGGATCTCTCAGAACCAATTCTGAGAGATCCAACTCCGAG-3′) were ligated into pSRG (pSUPERretro-IRES-hrGFP) vector plasmids. The 21-nucleotide RNA oligonucleotides of *Daxx* (sc-35178) and *Pml* (sc-36284) were purchased from Santa Cruz Biotechnology and were transfected into cells using Lipofectamine 2000 (Invitrogen).

Daxx-overexpressing and Daxx RNAi Ovarian Cancer Cell Lines—Ovarian cancer cells (ES-2, A2780, and SKOV-3) that stably expressed EGFP-DAXX and *Daxx* shRNA (si*Daxx*) were established as described previously (9). Briefly, cells were seeded in 60-mm dishes and transfected with 4 μg of pLEGFP-*Daxx* or pSuper-sh*Daxx* plasmids using Lipofectamine 2000. Cells with EGFP fluorescence were selected and cultured in complete cell culture medium along with either G418 (200 μg/ml) or puromycin (1 μg/ml) for 7–10 days.

Soft Agar Colony Assay—Cells were cultured using the method of Hamburger and Salmon (17) with modifications. One-milliliter layers of 0.5% agar were prepared in a 35-mm cell culture dish (Corning). Cells to be tested were suspended in 1 ml of 0.35% agar containing 1× cell culture medium and 10% fetal bovine serum and poured over these underlayers. The final cell concentration in each culture was 6×10^3 cells/ml. Triplicate cultures were used for each experiment. The plates were placed in a 5% CO_2 humidified incubator at 37 °C. Colonies were counted at 6 weeks after plating using an Omnicon FAS II Image Analysis System.

Wound Healing Assay—ES-2 cells (sh-control and sh*Daxx*- and GFP-DAXX-expressing cells) were grown to confluence in DMEM supplemented with 10% FBS. Then the medium was changed to FBS-free DMEM, and the cell monolayers were scraped in a straight line using a P-200 pipette tip to create a "scratch wound." The plates were photographed at 0 and 24 h using a phase contrast inverted microscope (Nikon Ti, Nikon Corp.).

Transwell Migration Assay—Twenty four-well tissue culture plate inserts with 8-μm pore filters and BioCoat Matrigel (BD Biosciences) were used to assess the migration and invasive potential of ES-2 cells that had been stably transfected with either control siRNA, sh*Daxx*, or GFP-*Daxx*. Cells were suspended in serum-free medium, and then added to a transwell (100-μl cell suspension/well at a concentration of $0.5–1 \times 10^5$ cells/ml). After incubation for 24 h at 37 °C, cells at the upper surface of the transwell were removed with cotton swabs. Cells that had migrated were attached to the lower surface and were stained with hematoxylin and eosin. Transwells were rinsed with water and air-dried. Positive cells were quantified using Image-Pro Plus 6.0 software.

Cell Growth Assay—ES-2 cells (sh-control and sh*Daxx*- and GFP-*Daxx*-expressing cells) were seeded in 96-well plates at 3×10^3/well in DMEM containing 10% FBS. After they adhered, cells were treated with 5 μg/ml bleomycin for 24 h and assessed for growth using an MTT assay. Briefly, 20 μl of MTT solution (5 mg/ml in PBS) was added into triplicate wells, and cells were incubated for 4–6 h in an incubator. Absorbance at 490 nm was read with a microplate reader.

RNA Isolation and Quantitative RT-PCR—Total RNA was isolated from tissues or cultured cells using TRIzol reagent (Invitrogen) following the manufacturer's protocols. Total RNA (5 μg) was reverse-transcribed using a cDNA synthesis kit (Bio-Rad). The following primers were used to amplify target genes: actin, 5′-GCTCTTTTCCAGCCTTCCTT-3′; 5′-GTACTTGCGCTCAGGAGGAG-3′; Daxx, 5′-TCTACAACTTTGGCTGTCACCTC-3′; 5′-GTCTCTTCTGTCTCTCGCCCT-3′; and Pml, 5′-GCTGACCCCCAAGCAGAAGA-3′; 5′-CTCAGAAAGCTGAGGAAGTGCTG-3′.

Immunohistochemistry—Paraffin-embedded human tissues from ovarian tumors and normal ovaries were provided by the Second Hospital of Jiaxing and the Jiaxing Maternity and Child Health Care Hospital, China. The use of archived cancer sam-

ples in this study was approved by the Zhejiang University Institutional Review Board.

Sections were cut with a Leica RM2235 microtome at 5 μm thicknesses and stained with affinity-purified anti-DAXX (Sigma) and anti-PML (Santa Cruz Biotechnology) antibodies for immunohistochemistry using a Vector ABC kit (Vector Laboratories). Briefly, sections were deparaffinized, rehydrated, and incubated in 0.3% H_2O_2. After antigen retrieval using 10 mM sodium citrate (pH 6.0), sections were incubated in normal goat serum. The samples were then probed with primary antibodies. After washing with PBS containing 0.05% Tween 20 (PBS-T), samples were incubated with a secondary antibody and washed again with PBS-T before incubation with ABC solution. Color was developed with a diaminobenzidine substrate kit (Vector Laboratories). The sections were washed, counterstained, dehydrated, and mounted with VectaMount permanent mounting medium (Vector Laboratories). Sections were viewed under a Nikon Eclipse 80i Microscope (Nikon Corp.). Staining intensity for DAXX and PML was scored by a pathologist (L. Guo).

Immunofluorescence—Tumor tissues were fixed in 4% paraformaldehyde, embedded in O.C.T. compound (Sakura Finetek USA Inc.), and stored at −80 °C before preparing 7-μm sections using a Leica CM1850 cryomicrotome (Leica Microsystems, Wetzlar, Germany). Cultured cells were seeded on coverslips and transfected with the desired plasmids. 24 h later, cells were washed with PBS, fixed with 4% paraformaldehyde, permeabilized with PBS containing 0.3% Triton X-100 (PBST), and incubated with blocking buffer (PBST containing 5% bovine serum albumin). Sections or cells were sequentially probed with primary antibodies as indicated under "Results" and Alexa Fluor 594- or 488-conjugated secondary antibodies (Molecular Probes). Slides were mounted using VectaShield with 4′,6-diamidino-2-phenylindole (DAPI, Vector Laboratories). Digital images were acquired using an epifluorescence microscope (Nikon Eclipse 80i) with 4–100× objectives.

Western Blot Analysis—Cell extracts containing 30 μg of protein were resolved by SDS-PAGE and transferred to PVDF membranes (Millipore Corp., Bedford, MA). After probing with primary antibodies, the membranes were incubated with horseradish peroxidase-linked anti-rabbit antibodies (Cell Signaling Technologies, Danvers, MA) and then washed. Bound antibodies were visualized using an enhanced chemiluminescence detection kit (Amersham Biosciences). The primary antibodies were as follows: DAXX (Sigma), p-H2AX (Ser-139), p-CHK1 (Ser-345), p-Chk2 (Thr-68), p-histone H3 (Ser-10), cleave caspase 3, β-actin (Cell Signaling), p27, GFP, PML (Santa Cruz Biotechnology), and collagen IV (Abcam).

Statistical Analysis—All *in vitro* assays were performed in triplicate. Groups were compared by two-tailed *t* tests or analysis of variance using GraphPad Prism statistical programs (GraphPad Prism, San Diego). $p < 0.05$ was considered significant.

RESULTS

DAXX Is Overexpressed in Human Ovarian Cancer Tissues and Cell Lines—DAXX protein expression in human tissues was assessed by immunohistochemistry. As shown in Fig. 1, *A* and *B* (*left panels*), DAXX was weakly expressed in normal ovarian tissue. Significant DAXX staining intensity was detected in endometrioid carcinoma (92.3%), serous cystadenoma (91.7%), clear cell carcinoma (100%), and mucinous cystadenoma (100%), whereas DAXX was only weakly expressed in granular cell tumor tissues (0%) (Table 1). The subcellular localization of DAXX was also examined in ovarian cancer cell lines. DAXX was localized in nuclei and formed nuclear foci in most ovarian cancer cell lines (ES-2, C13, SKOV-3, and A2780; Fig. 1*C*). Interestingly, more cytoplasmic DAXX signals were detected in immortalized ovarian surface epithelial cells (mOSE) and HeLa cervical cancer cells.

The relative *Daxx* mRNA expression levels in ovarian cancer cells and other ovarian cell types were determined by real time PCR. *Daxx* mRNA was highly expressed in human ovarian cancer cells, mOSE cells, and oocytes, but it was weakly expressed in granulosa cells, the most abundant cell type in the ovary (Fig. 1*D*). At the protein level, as compared with other tissues, DAXX was highly expressed in reproductive organs (uterus, testis, and ovary; Fig. 1*E*). The expressions of *Daxx* mRNA and protein at high levels in ovarian cancer tissues and ovarian cancer cell lines suggested that *Daxx* could play an essential role in ovarian tumor cell proliferation and migration.

To investigate a role for *Daxx* in ovarian cancer cells, we developed ovarian cancer cell lines (ES-2) that stably expressed shRNA that targeted *Daxx* sequences (designated shRNA2 and shRNA3). *Daxx* was efficiently knocked down in these cell lines, as shown by quantitative real time PCR and Western blot (Fig. 1*F*). We also developed ovarian cancer cell lines that stably overexpressed GFP-tagged DAXX. GFP-DAXX fusion protein expression and its nuclear localization were established by Western blotting and immunofluorescence, respectively (Fig. 1, *G* and *H*).

Daxx Promotes Ovarian Cancer Cell Survival and Metastasis—First, we investigated roles for *Daxx* in the survival, proliferation, and migration of ovarian cancer cells. As shown in Fig. 2*A*, GFP-DAXX-overexpressing ES-2 cells grew faster than control cells, whereas *Daxx* silencing remarkably reduced cell growth as assessed by MTT assays. In addition, *Daxx* silencing remarkably inhibited the growth of other human ovarian cancer cell lines, including OV2008 and SKOV3 (data not shown). Furthermore, DAXX overexpression in ES-2 and SKOV3 cells significantly promoted colony formation in soft agar and increased the sizes of these colonies (Fig. 2, *B* and *C*). Immunofluorescent staining and Western blotting of cleaved caspase 3 (Fig. 2, *D* and *E*) indicated that the numbers of apoptotic cells were dramatically increased after RNAi depletion of *Daxx* or *Pml*. We also generated mock stable cell lines (expressing GFP) as the control when we studied overexpressed GFP-DAXX. GFP-expressing ovarian cancer cells did not show any differences from nontransfected cells in cell growth and clone formation assays (supplemental Fig. 1).

The effect of *Daxx* on ovarian cancer cell migration was also determined. Using a scratch wound assay, DAXX overexpression noticeably promoted the migration of ES-2 cells, whereas *Daxx* silencing inhibited the migration of these cells (Fig. 2*F*). In another experiment, we examined *Daxx*-stimulated ovarian cancer ES-2 cells' metastatic potential using a transwell assay.

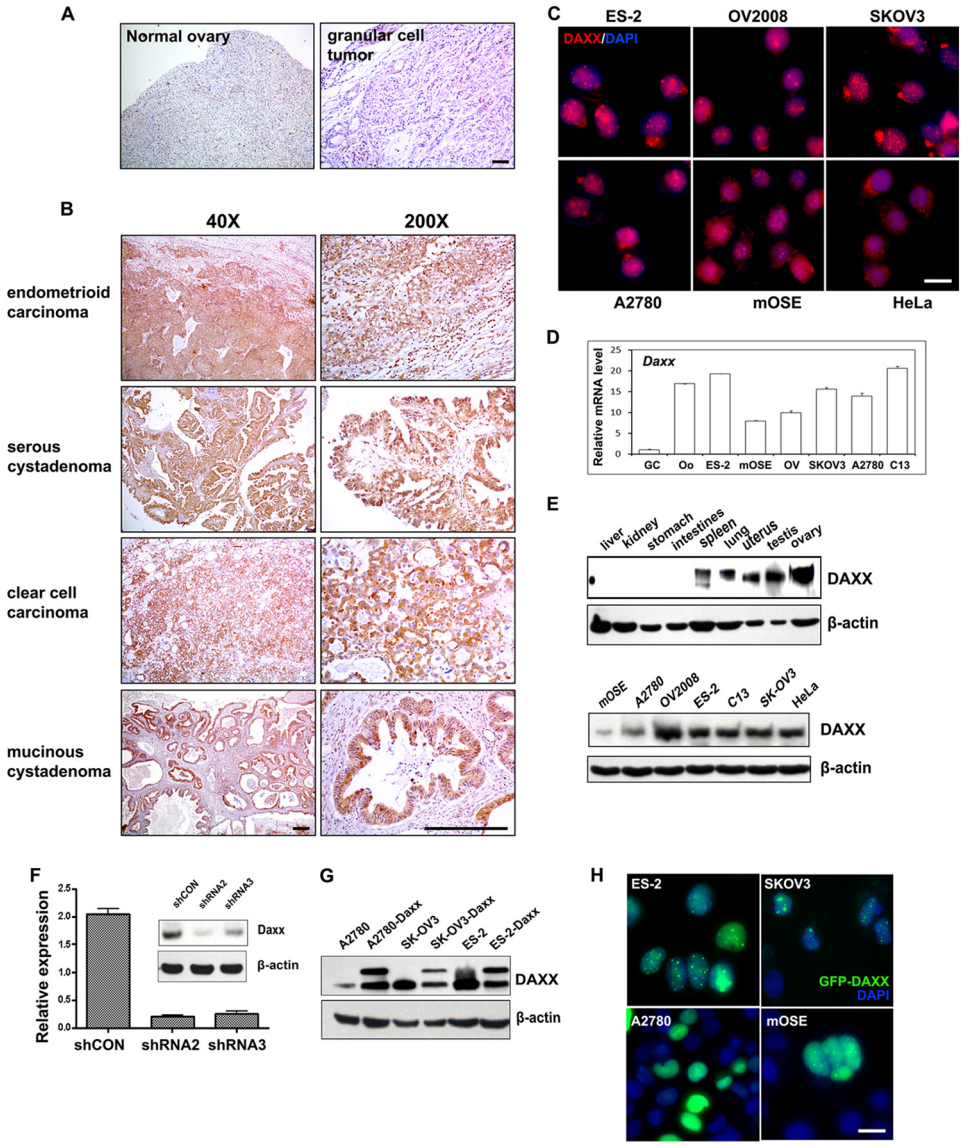

FIGURE 1. **DAXX expression patterns in human ovarian cancer samples and cell lines.** *A* and *B,* immunohistochemistry results for DAXX expression in normal human ovary and ovarian cancer tissues. Sections were counterstained with hematoxylin. *Scale bar,* 200 μm. *C,* DAXX immunofluorescent staining in cultured ovarian cancer cells (ES-2, OV2008, SKOV3, and A2780), immortalized mOSE cells, and HeLa cells. Cells were seeded on glass coverslips in 24-well plates overnight before staining. Nuclei were visualized by 4′,6′-diamidino-2-phenylindole (DAPI) staining (*blue*). *Scale bar,* 10 μm. *D,* quantitative RT-PCR for *Daxx* mRNA expression levels in cultured ovarian cancer cells, mouse oocyte, and granular cells. *E,* Western blot analysis for DAXX protein expression levels in mouse tissues and cultured cell lines. *β*-Actin was used as the loading control. *F,* quantitative RT-PCR and Western blot results for the effects of *Daxx* silencing with RNAi. ES-2 cells were transfected with either control shRNA (*shCON*), *Daxx*-shRNA2, or *Daxx*-shRNA3; total mRNAs and proteins were isolated 48 h after transfection. *G,* Western blot results showing stable overexpression of DAXX protein in ovarian cancer cells. Ovarian cancer cells (A2780, ES-2, and SKOV3) were transfected with pLEGFP-*Daxx* and selected with G418 for more than 2 weeks. *H,* fluorescence microscopy results for the localization of overexpressed DAXX (*green*) in ovarian cancer cells (ES-2, SKOV3, and A2780) and mOSE cells that were stably transfected with GFP-*Daxx*. Nuclei were stained with DAPI (*blue*). *Scale bar,* 10 μm.

TABLE 1
DAXX protein expression in ovarian cancer and normal ovary tissues

Pathological classification	Total patients	Cases with high levels of DAXX expression	*N* (patients)
			%
Normal ovary tissue	3	0	0
Serous cystadenoma	36	33	91.7
Endometrioid carcinoma	13	12	92.3
Clear cell carcinoma	3	3	100
Mucinous cystadenoma	4	4	100
Granular cell tumor	3	0	0

The migration of ES-2 cells was increased by 2-fold due to DAXX overexpression, but it was significantly decreased by *Daxx* silencing (Fig. 2*G*). These results demonstrated that *Daxx* was required for ovarian cancer cell proliferation and migration.

Daxx Promotes the Tumorigenic Capacity of Ovarian Cancer Cells in Vivo—We also investigated roles for *Daxx* in ovarian cancer cell proliferation and metastasis *in vivo*. Female athymic nude mice were injected intraperitoneally with either control ES-2 cells or ES-2 cells that stably expressed GFP-DAXX (ES-2+*Daxx*) or *Daxx*-shRNA (ES-2 sh*Daxx*). Nude mice that received ES-2+*Daxx* cells showed visible abdominal distention and had accumulated large amounts of ascites at 30 days (Fig. 3*A*).

These ascites cells were harvested and cultured in standard DMEM containing 10% FBS. Cytological examination revealed that most of these ascites cells were positive for GFP (Fig. 3*B*),

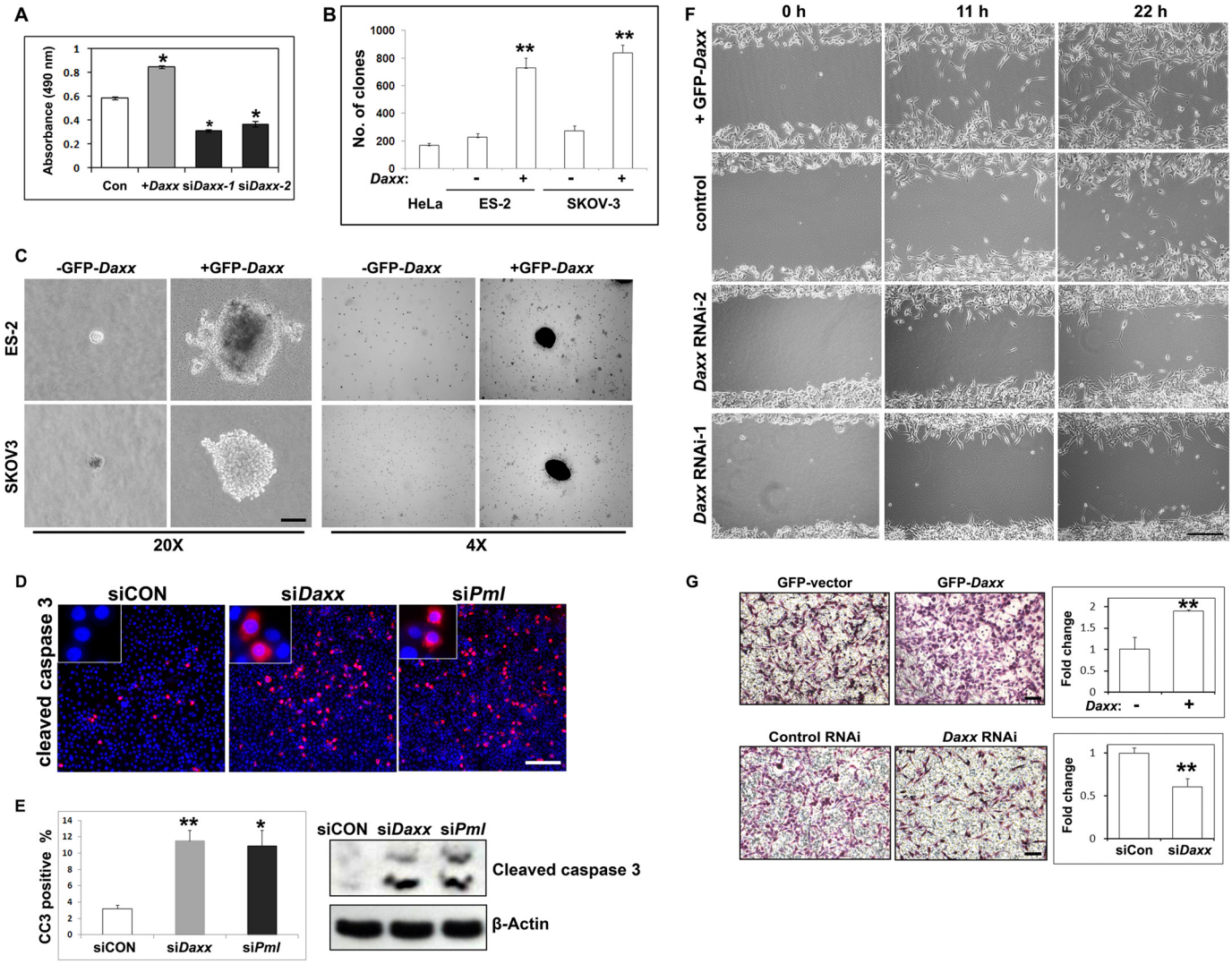

FIGURE 2. **DAXX promotes ovarian cancer cell colony formation and migration.** *A,* DAXX-induced ovarian cancer cell proliferation. Cells were seeded into 96-well plates (3,000 cells/well) overnight, treated with 5 μg/ml bleomycin for 24 h, and then assessed by MTT assay. *B* and *C,* colony formation assay for the growth of ES-2 and SKOV3 cells, with or without *Daxx* overexpression. Cells were cultured in Matrigel. Colonies that formed at days 40 are shown. Colony numbers were counted at day 40. *Scale bar,* 100 μm. *D,* immunofluorescent staining of cleaved caspase 3 after RNAi depletion of *Daxx* or *Pml*. *Scale bar,* 100 μm. *E,* quantification of cleaved caspase 3-positive cells in *D,* and Western blotting results showing the levels of cleaved caspase 3 with or without *Daxx*/*Pml* RNAi. *F,* wound-healing assay for the migration capability of ES-2 cells and their derivatives (GFP-*Daxx* overexpression and si*Daxx* stable cell lines) cultured in serum-free medium. *Scale bar,* 100 μm. *G,* transwell experiment for the migration capability of ES-2 cells and their derivatives (GFP-*Daxx* overexpression and si*Daxx* stable cell lines). Cells were added to transwells and allowed to migrate for 12 h. Cells at the upper surface of the membrane were removed with cotton swabs, and the cells on the bottom surface were stained with hematoxylin and eosin. Numbers of cells (*Daxx*-overexpressing group or *Daxx*-depleted group) on the bottom surface were counted and were compared with the control group (set as 1). *, $p < 0.01$; **, $p < 0.001$. *Scale bar,* 50 μm.

which indicated that they were derived from the transplanted ES-2+*Daxx* cells. These cells could be grown and passaged indefinitely *in vitro* (data not shown). In addition, the weights of the abdominal solid tumors formed by ES-2+*Daxx* cells were 3-fold greater than the weights of control tumors formed by the original ES-2 cells (Fig. 3*A*). In contrast, RNAi silencing of *Daxx* dramatically inhibited the growth of these transplanted cancer cells (Fig. 3*A*).

Examining the peritoneal cavities of mice that had received ES-2+*Daxx* cells revealed dramatic, diffuse studding of tumor deposits on the liver and intestine (Fig. 3*C*). By comparison, control ES-2 cells resulted in the formation of fewer diffuse colonies in these tissues. In addition, *Daxx*-depleted ES-2 cells failed to form any metastasized colonies in the peritoneal cavity (Fig. 3*C*). Immunohistochemical examination confirmed that DAXX and PML were highly expressed in ES-2+*Daxx* tumors, but their expressions were dramatically decreased in ES-2 sh*Daxx* tumors (Fig. 3*F*). Significant cell proliferation was only detected in ES-2-*Daxx* tumors by immunostaining for phosphohistone H3. However, ES-2 sh*Daxx* tumors contained noticeable amounts of apoptotic cells, as shown by immunostaining for cleaved caspase 3 (Fig. 3*F*).

To assess the effect of *Daxx* on tumor cell growth, we next implanted ES-2 and ES-2+*Daxx* cells and SKOV3 and SKOV3+*Daxx* cells subcutaneously into the left and right flanks of nude mice, respectively. As shown in Fig. 3*D*, tumors that formed due to *Daxx*-overexpressing cells were significantly larger than those formed due to control cells. Fluorescent microscopy for GFP confirmed that the majority of the tumor cells were derived from GFP-DAXX-expressing cells

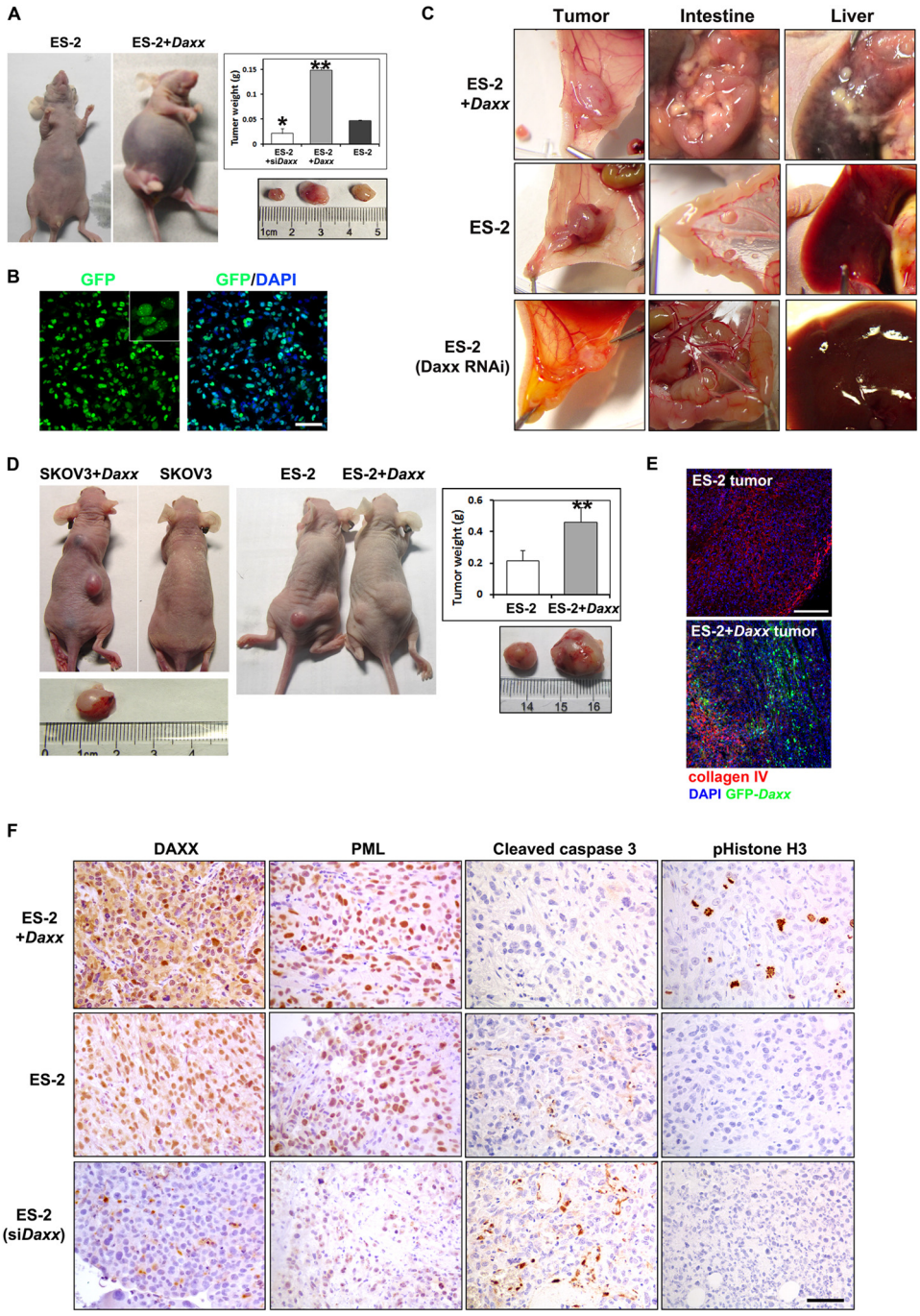

FIGURE 3. **DAXX promotes ovarian cancer cell proliferation and metastasis *in vivo*.** *A*, ES-2 cells and their derivatives (GFP-*Daxx* overexpression and si*Daxx* stable cell lines) were injected intraperitoneally into nude mice (10^6 cells/mouse). After 30 days, mice that received Daxx-overexpressing ES-2 cells had significant ascites accumulation. Tumors were removed and weighed ($n = 18$). Results are the means ± S.E. of six independent experiments. *B*, ascites fluid cells were harvested from nude mice and cultured *in vitro*. Abundant GFP signals were observed by fluorescent microscopy. *Left panel*, GFP. *Right panel*, merge (GFP and DAPI). *Scale bar*, 50 μm. *C*, ES-2 cells and their derivatives (GFP-Daxx overexpression and siDaxx stable cell lines) were injected underneath the abdomen membrane of nude mice (10^6 cells/mouse). *In situ* colonization of tumor cells and metastasis to the intestine and liver were examined 3 weeks later. *D*, ovarian cancer cells (SKOV3 and ES-2) with or without DAXX overexpression (10^6 cells for each) were implanted subcutaneously into different nude mice, respectively. After 30 days, tumors were removed and weighed ($n = 10$). *E*, cryosections were prepared from tumor tissues derived from ES-2 and DAXX-overexpressing ES-2 cells. Prominent angiogenesis was shown by immunofluorescent staining for collagen IV (*red*). DAXX overexpression was shown by GFP fluorescence (*green*). Tissues were counterstained with DAPI (*blue*). *Scale bar*, 100 μm. *F*, immunohistochemistry staining for DAXX, PML, cleaved caspase3, and pHistone H3 in representative ES-2-derived tumor tissues. *Scale bar*, 50 μm.

(Fig. 3*E*). The tumor tissues were co-stained with an antibody against collagen IV to demonstrate tumor angiogenesis. Taken together, these results demonstrated that *Daxx* was required for growth and metastasis *in vivo* of ovarian cancer cells.

Daxx Induces Tumorigenic Transformation in Normal Ovarian Surface Epithelial Cells—To determine whether *Daxx* overexpression could also induce tumor formation by normal OSE cells, we generated an immortalized mouse OSE cell line that stably expressed GFP-DAXX (Fig. 4*A*). Then mOSE cells, with

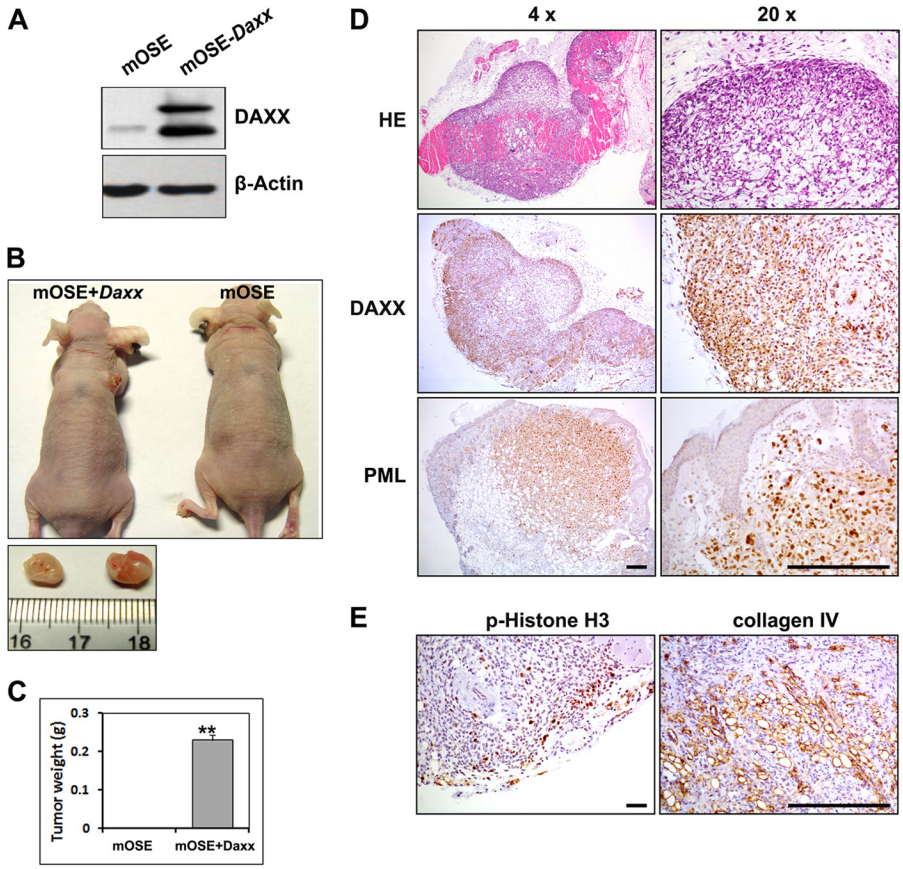

FIGURE 4. **Nontumorigenic ovarian surface epithelial cells are transformed by Daxx overexpression.** *A,* Western blot results for DAXX overexpression in immortalized OSE cells. *B* and *C,* mOSE and mOSE-*Daxx* cells (10^6 cells for each) were implanted subcutaneously into different nude mice, respectively. After 60 days, tumors were removed and weighed ($n = 10$). *D,* immunohistochemical staining for the DAXX and PML expression levels in mOSE-Daxx tumor tissues. *Scale bar,* 200 μm. *E,* immunohistochemical staining for pHistone H3 (pHH3) and collagen IV showing active cell proliferation and angiogenesis in mOSE-*Daxx* tumor tissues. *Scale bar,* 200 μm; **, $p < 0.001$.

or without *Daxx* overexpression, were subcutaneously implanted into the flanks of nude mice. As shown in Fig. 4, *B* and *C*, after 60 days, tumor formation was detected in the mice that had received mOSE+*Daxx* cells but not in control mice that had received normal mOSE cells. DAXX and PML proteins were highly expressed in tumor xenografts, as determined by immunohistochemistry (Fig. 4*D*). The cell proliferation marker phosphohistone H3 and the endothelial cell marker collagen IV were also highly expressed in tumor xenografts (Fig. 4*E*), which indicated that the grafted tissue was highly proliferative and angiogenic. These results suggested that *Daxx* possessed oncogenic characteristics in normal OSE cells; when overexpressed, *Daxx* could induce tumorigenic transformation in this cell type.

Daxx Protects Ovarian Cancer Cells against X-ray Irradiation-induced DNA Damage—Cellular resistance to radiotherapy and chemotherapy remains one of the greatest unresolved problems in treating ovarian cancer. Previous reports suggested that *Daxx* participated in DNA damage signaling in apoptosis (18). H2AX and CHK1/2 phosphorylation is an essential early step in DNA damage responses. X-ray irradiation induced dramatic DNA damage responses in ES-2 cells, as demonstrated by immunostaining for phospho-H2AX (pH2AX) and phospho-CHK2 (pCHK2; Fig. 5*A*). However, cells that were transfected with si*Daxx* had high levels of pH2AX and pCHK2, even without x-ray irradiation (Fig. 5, *B–D*). Furthermore, when exposed to x-ray irradiation, GFP-DAXX-overexpressing cells displayed less H2AX/CHK2 phosphorylation than the adjacent GFP-DAXX negative cells, whereas *Daxx* knockdown cells displayed more dramatic H2AX/CHK2 phosphorylation than the control cells in the same fields of view (Fig. 5, *B–D*). Western blotting analysis also showed that pH2AX levels were decreased by *Daxx* overexpression before and after x-ray irradiation (Fig. 5*E*).

Next, we examined the time-dependent effect of DAXX on x-ray irradiation-induced DNA damage. As expected, x-ray irradiation induced rapid DNA damage within 5 min (data not shown). DAXX overexpression in ES-2 cells significantly suppressed x-ray irradiation-induced H2AX and CHK1 phosphorylation at all time points examined (Fig. 5*F*). In contrast, *Daxx* RNAi further enhanced H2AX/CHK1 phosphorylation after x-ray irradiation (Fig. 5*G*). Taken together, these results suggested that *Daxx* protected ovarian cancer cells from DNA damage after exposure to x-ray irradiation.

DAXX and PML Protect Ovarian Cancer Cells from DNA Damage Responses Induced by Chemotherapy—Because of its known cellular effect of causing DNA double strand breaks, the widely used chemotherapy drug BLM (20 μg/ml) also induced dramatic H2AX and CHK2 phosphorylation in ovarian cancer cells (Fig. 6*A*). In addition, DAXX and PML nuclear foci dramatically increased after BLM treatment in a time-dependent manner (Fig. 6, *B* and *C*). Immunostaining for pH2AX, pCHK2,

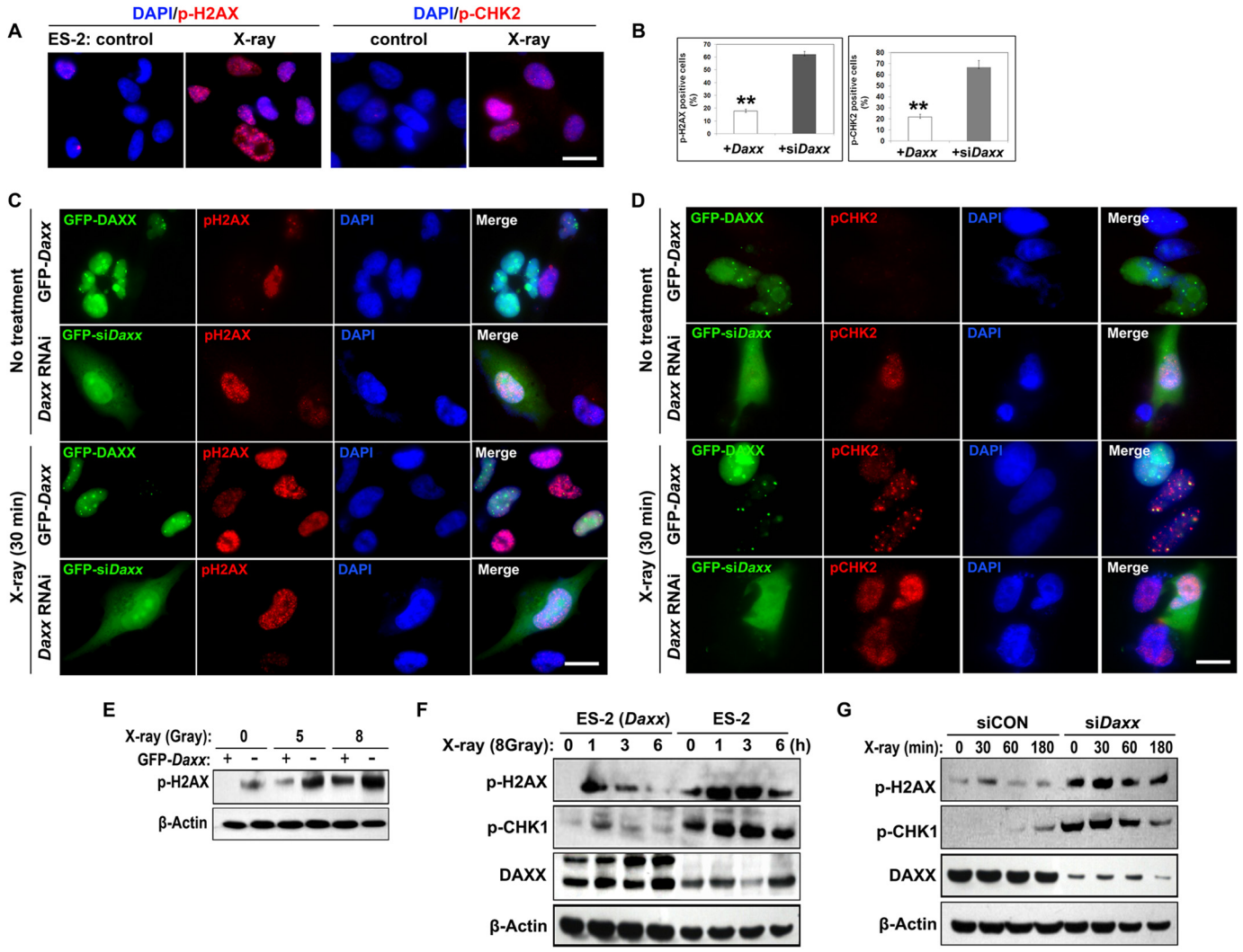

FIGURE 5. **DAXX protects ovarian cancer cells against DNA damage insults.** *A,* immunofluorescence results showing increased pH2AX and pCHK2 in ES-2 cells after x-ray irradiation. *Scale bar,* 10 μm for all images. *B,* percentages of *Daxx*-overexpressing or *Daxx*-depleted cells that were positive for p-H2AX and p-CHK2. **, $p < 0.001$. *C* and *D,* immunofluorescence results for the levels of pH2AX and pCHK2 in *Daxx*-overexpressing or *Daxx*-depleted ES-2 cells, with or without x-ray treatment (8 gray). *Green,* GFP-labeled *Daxx* overexpressing or *Daxx*-depleted cells; *red,* p-H2AX and p-CHK2; *blue,* DNA stained with DAPI. *E,* Western blot results for the dose-dependent induction of H2AX phosphorylation by x-ray irradiation (0, 5, and 8 gray) in ES-2 cells, with or without overexpressed GFP-DAXX. *F* and *G,* Western blot results for x-ray irradiation-induced phosphorylation of H2AX and CHK1 in ES-2 cells and their derivatives (ES-2-GFP-*Daxx* and ES-2-si*Daxx*). Cells were harvested at the indicated times (hours) after x-ray irradiation (8 gray).

and PML in GFP-*Daxx*-expressing ES-2 cells indicated that pH2AX and pCHK2 partially co-localized with DAXX after DNA damage (Fig. 6*A*) and that PML co-localized with DAXX in most nuclear foci (Fig. 6*B*). An ~4-fold increase in PML foci was detected at 12 h after BLM treatment (Fig. 6*C*). In addition, DAXX and PML protein levels were notably increased in ES-2 cells after BLM treatment (Fig. 6*D*). These results suggest that DAXX-PML nuclear bodies are highly dynamic and increase after DNA damage.

DAXX Protects Ovarian Cancer Cells from DNA Damage Insults by Interacting with PML—The subcellular distribution of PML was almost similar to that of DAXX in these ovarian cancer cell lines (supplemental Fig. 1*D*). Because DAXX co-localized with PML in ovarian cancer cells during DNA damage responses, we investigated the PML protein expression in normal mouse ovary and human ovarian tumor tissue by immunohistochemistry. As shown in Fig. 6*E*, PML was weakly expressed in the surface epithelium of mouse ovary and in human granular cell tumors. However, significant PML expression was detected in all OSE cancer samples.

To investigate a role for PML in DNA damage processes, we depleted PML by siRNA (si*Pml*) and analyzed the effects on DNA damage by immunofluorescence. Endogenous DAXX and PML were detected in the nuclei of control cells (Fig. 6*F*). However, both DAXX and PML expressions were significantly decreased in si*Daxx* and si*Pml* cells (Fig. 6, *F* and *G*). The percentage of p-H2AX-positive cells significantly increased from 1.6% (siCON) to 14.3% (si*Pml*) without any additional DNA damage insults (Fig. 6, *F* and *I*). As expected, x-ray irradiation induced an increase in pH2AX signals in cells that were transfected with siCON. However, a more dramatic increase in pH2AX-positive cells was found after si*Daxx* and si*Pml* transfections. DAXX, PML, and p-H2AX protein levels in ovarian cancer cells were examined by Western blot after x-ray irradiation (Fig. 6*H*). Both PML and DAXX protein levels were reduced in si*Pml* cells due to PML depletion, with or without

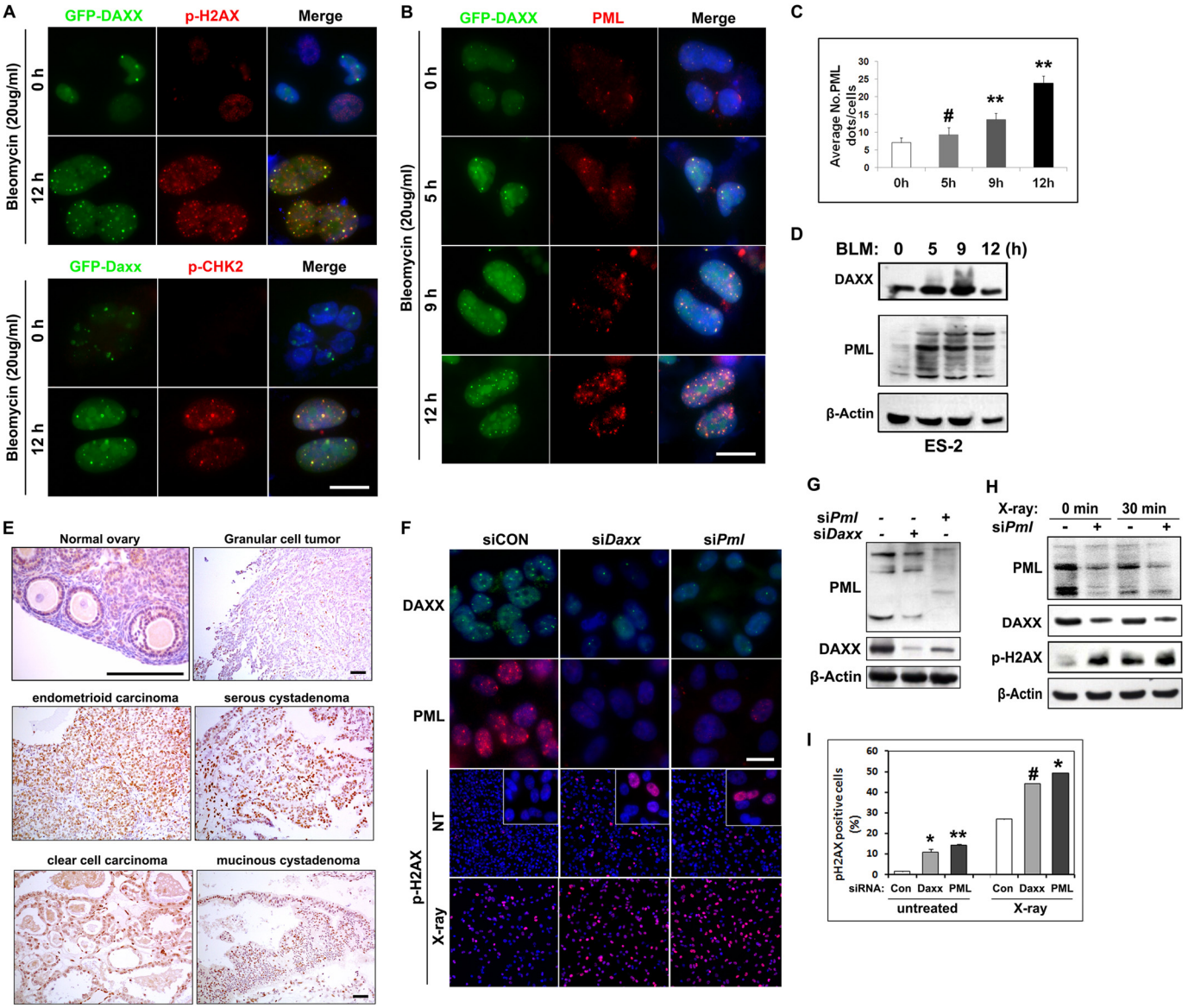

FIGURE 6. **DAXX cooperates with PML in ovarian cancer cells in response to DNA damage insults.** *A* and *B*, immunofluorescence results for nuclear pH2AX, pCHK2, and PML foci formation after bleomycin treatment. ES-2 cells that stably expressed GFP-DAXX fusion proteins were treated with bleomycin (20 μg/ml) for 0, 5, 9, and 12 h. *Scale bar*, 10 μm. *C*, quantification of PML foci in nuclei after bleomycin treatment at the indicated times. *D*, Western blot results showing increased DAXX and PML protein levels after BLM treatment. *E*, PML expressions in normal ovary and ovarian cancer tissues were determined by immunohistochemistry. *Scale bar*, 200 μm. *F* and *G*, immunofluorescence staining (*F*) and Western blotting (*G*) for PML and DAXX in cells transfected with si*Daxx* and/or si*Pml*. Phospho-H2AX was detected by immunofluorescence before and after x-ray irradiation. *Scale bar*, 10 μm. *H*, Western blot results for PML RNAi-induced changes in DAXX and pH2AX. *I*, quantification of p-H2AX-positive cells in si*Pml* and si*Daxx*-treated cells, with or without x-ray irradiation. Shown is mean ± S.E. ($n = 3$): #, $p < 0.05$; *, $p < 0.01$; **, $p < 0.001$.

x-ray irradiation, whereas p-H2AX levels were significantly increased in si*Pml* cells both before and after x-ray irradiation. These results were in agreement with the results for immunofluorescent staining. Together, these results suggest that PML actively participates in DNA damage responses in ovarian cancer cells by interacting with DAXX.

DISCUSSION

Ovarian cancer is the most lethal type of gynecologic malignancy. The high mortality rate associated with this disease may be attributable to its late diagnosis and the complications that arise from metastasis (19). Unlike most carcinomas that rely on the vasculature for metastasis, an early event in ovarian cancer dissemination is the shedding of cells from the primary tumor into the peritoneal cavity followed by diffuse "seeding" of the peritoneal cavity (20). This unique metastatic mechanism presents a distinct set of therapeutic challenges. Additionally, successful treatment is limited by the high rate of chemoresistance in recurrent ovarian cancer. Research on the molecular bases of metastasis and chemoresistance are of the utmost importance for improving patient survival.

PML includes the scaffold component of PML-NBs and recruits a striking variety of proteins into these domains, including DAXX. Numerous studies have shown that PML and DAXX are involved in multiple aspects of nuclear functions, including transcription (21–24), DNA damage responses (25,

26), senescence (5, 27), apoptosis (28–30), and the regulation of nuclear organization (31–33). In ovarian surface epithelial cells and ovarian cancer cells, it is not known if the *Daxx* and *Pml* genes are transcribed or if PML-NBs are present. Thus, it has yet to be determined whether DAXX and PML proteins play important roles in ovarian cancer development. In this study, we report for the first time that DAXX is highly expressed in ovarian cancer cells and is actively involved in proliferation, metastasis, and DNA damage responses through its associations with PML-NBs.

DAXX functions as either a pro-apoptotic or an anti-apoptotic factor, depending on the cell type and context. Key evidence for a possible anti-apoptotic function of *Daxx* is derived from *Daxx* knock-out mouse embryos that displayed increased global apoptosis (6). In contrast, evidence for pro-apoptotic functions of DAXX was obtained with tumor cells or transformed cells that were treated with various stimuli, including UV light, TGF-β, hydrogen peroxide, interferon-γ, and arsenite trioxide (34). Thus, it has been suggested that DAXX exerts an anti-apoptotic activity in unstressed primary cells, whereas it is a pro-apoptotic factor in tumor cells or transformed cells exposed to various types of stress. Our study provides new evidence that, in both normal OSE cells and highly transformed ovarian cancer cells, DAXX promotes cell proliferation and represses DNA damage responses during x-ray irradiation and chemotherapy drug treatment and therefore may function as an anti-apoptotic factor. This is further suggested by the *in vivo* observation that the tumor tissues derived from DAXX-overexpressing ovarian cancer cells had decreased apoptosis signals (Fig. 3*F*).

In addition, DAXX depletion resulted in cell death and triggered DNA damage responses, which indicated that DAXX was required for maintaining genome integrity and suppressing DNA damage-induced apoptosis, which is critically important among rapidly proliferating ovarian cancer cells. Thus, DAXX may indirectly promote tumor development *in vivo* by suppressing a DNA damage checkpoint and apoptosis. DAXX might also interact with transcription regulators and directly stimulate proliferation in ovarian cancer cells, as has been reported for other cell types.

Within the nucleus, DAXX interacts with PML and localizes to PODs. It has been shown that DAXX localization within PODs is correlated with DAXX's pro-apoptotic or anti-apoptotic activity (34). For example, DAXX mutants that fail to localize within PODs do not facilitate FAS-induced cell death. Furthermore, in the absence of PML, DAXX is dispersed throughout the nucleus, and activated cell death is reduced. In this study, we observed that more nuclear PML bodies were formed in ovarian cancer cells after DNA damage insults and that DAXX-PML partially co-localized with the DNA damage markers pH2AX and pCHK2. Furthermore, similar to *Daxx* RNAi, PML depletion also resulted in genome instability in cultured ovarian cancer cells (Fig. 6, *F* and *H*). All of these results strongly suggest that DAXX protects ovarian cancer cells from DNA damage insults by interacting with PML.

We also observed that DAXX and PML protein levels were regulated as evidenced by the following. 1) In cells that stably expressing GFP-DAXX, the level of endogenous DAXX also increased (Fig. 5*F*). 2) BLM treatment induced not only the formation of PML and pH2AX foci but also resulted in increased DAXX and PML protein levels. We noticed that it took a relatively long time for DAXX protein levels to increase after a DNA damage insult (at least 24 h after BLM treatment). However, in Fig. 6*H*, DAXX protein levels did not change dramatically in cells treated with x-ray irradiation for only 30 min. In our experiments, a large proportion of cells were dying 24 h after x-ray irradiation, which made it technically difficult to evaluate the long term effect of x-ray irradiation on DAXX protein levels. 3) RNAi silencing of DAXX also caused a decrease in PML and vice versa. The detailed biochemical mechanism(s) underlying this mutual dependence remains unclear. We speculate that PML and DAXX may both be required for the organization or stabilization of PML nuclear bodies. Therefore, depleting one of them will affect the stability of the other one. This mutual dependence may help us to explain why both DAXX and PML expressions are low in normal ovarian tissues but are up-regulated in human ovarian cancer tissue. These multiple regulatory aspects for DAXX and PML reflect the importance and complexity of their functions in ovarian cancer cells. However, it remains unclear if this regulation occurs at the transcriptional level or the post-translational level. Thus, further investigation is required.

Our results for DAXX expression in OSE and ovarian cancer cells also have clinical and therapeutic implications. 1) DAXX and PML protein levels were decreased in many cancer tissues but were dramatically increased in ovarian surface epithelial cancer tissues. Interestingly, ovarian granulosa cell tumors, which belong to another major ovarian cancer type, were negative for DAXX and PML. Therefore, DAXX and PML detection may be a new approach for a clinical diagnosis of ovarian cancers. 2) Depleting DAXX suppressed the tumorigenic capacity of ovarian cancer cells *in vivo* and increased their sensitivity to DNA-damaging insults, including x-irradiation and bleomycin treatment. Thus, small molecules that can inhibit DAXX activity or DAXX accumulation may have the therapeutic potential to enhance the effects of radiotherapy and chemotherapy for ovarian cancer patients. 3) The DAXX expression level was relatively low in normal OSE cells, and DAXX overexpression resulted in tumorigenic transformation in this cell type. This was consistent with the observation of DAXX overexpression in human ovarian cancer samples. These results indicate that DAXX up-regulation might be a key step in initiating ovarian cancer and could possibly be used as an early diagnostic marker for ovarian cancers.

Acknowledgments—We thank Dr. Karl-Heinz Klempnauer for the GFP-Daxx-expressing plasmid. We also thank Drs. Kunliang Guan and Reihua Chen for helpful discussions.

REFERENCES

1. Abedini, M. R., Muller, E. J., Brun, J., Bergeron, R., Gray, D. A., and Tsang, B. K. (2008) Cisplatin induces p53-dependent FLICE-like inhibitory protein ubiquitination in ovarian cancer cells. *Cancer Res.* **68,** 4511–4517
2. Abedini, M. R., Muller, E. J., Bergeron, R., Gray, D. A., and Tsang, B. K. (2010) Akt promotes chemoresistance in human ovarian cancer cells by modulating cisplatin-induced, p53-dependent ubiquitination of FLICE-

like inhibitory protein. *Oncogene* **29,** 11–25
3. Abedini, M. R., Qiu, Q., Yan, X., and Tsang, B. K. (2004) Possible role of FLICE-like inhibitory protein (FLIP) in chemoresistant ovarian cancer cells *in vitro*. *Oncogene* **23,** 6997–7004
4. Yang, X., Khosravi-Far, R., Chang, H. Y., and Baltimore, D. (1997) Daxx, a novel Fas-binding protein that activates JNK and apoptosis. *Cell* **89,** 1067–1076
5. Chen, L. Y., and Chen, J. D. (2003) Daxx silencing sensitizes cells to multiple apoptotic pathways. *Mol. Cell. Biol.* **23,** 7108–7121
6. Michaelson, J. S., Bader, D., Kuo, F., Kozak, C., and Leder, P. (1999) Loss of Daxx, a promiscuously interacting protein, results in extensive apoptosis in early mouse development. *Genes Dev.* **13,** 1918–1923
7. Salomoni, P., and Khelifi, A. F. (2006) Daxx: death or survival protein? *Trends Cell Biol.* **16,** 97–104
8. Morozov, V. M., Massoll, N. A., Vladimirova, O. V., Maul, G. G., and Ishov, A. M. (2008) Regulation of c-met expression by transcription repressor Daxx. *Oncogene* **27,** 2177–2186
9. Wethkamp, N., and Klempnauer, K. H. (2009) Daxx is a transcriptional repressor of CCAAT/enhancer-binding protein β. *J. Biol. Chem.* **284,** 28783–28794
10. Lin, D. Y., Lai, M. Z., Ann, D. K., and Shih, H. M. (2003) Promyelocytic leukemia protein (PML) functions as a glucocorticoid receptor co-activator by sequestering Daxx to the PML oncogenic domains (PODs) to enhance its transactivation potential. *J. Biol. Chem.* **278,** 15958–15965
11. Chang, C. C., Lin, D. Y., Fang, H. I., Chen, R. H., and Shih, H. M. (2005) Daxx mediates the small ubiquitin-like modifier-dependent transcriptional repression of Smad4. *J. Biol. Chem.* **280,** 10164–10173
12. Yeung, P. L., Chen, L. Y., Tsai, S. C., Zhang, A., and Chen, J. D. (2008) Daxx contains two nuclear localization signals and interacts with importin α3. *J. Cell. Biochem.* **103,** 456–470
13. Takahashi, Y., Lallemand-Breitenbach, V., Zhu, J., and de Thé, H. (2004) PML nuclear bodies and apoptosis. *Oncogene* **23,** 2819–2824
14. Hofmann, T. G., and Will, H. (2003) Body language: the function of PML nuclear bodies in apoptosis regulation. *Cell Death Differ.* **10,** 1290–1299
15. Lv, L., Zhang, T., Yi, Q., Huang, Y., Wang, Z., Hou, H., Zhang, H., Zheng, W., Hao, Q., Guo, Z., Cooke, H. J., and Shi, Q. (2012) Tetraploid cells from cytokinesis failure induce aneuploidy and spontaneous transformation of mouse ovarian surface epithelial cells. *Cell Cycle* **11,** 2864–2875
16. Mullany, L. K., Fan, H. Y., Liu, Z., White, L. D., Marshall, A., Gunaratne, P., Anderson, M. L., Creighton, C. J., Xin, L., Deavers, M., Wong, K. K., and Richards, J. S. (2011) Molecular and functional characteristics of ovarian surface epithelial cells transformed by KrasG12D and loss of Pten in a mouse model *in vivo*. *Oncogene* **30,** 3522–3536
17. Tveit, K. M., Kaern, J., Hoifodt, H. K., Pettersen, E. O., Abeler, V., Davy, M., Hannisdal, E., and Trope, C. (1989) Colony-forming ability of human ovarian carcinomas in the Courtenay soft agar assay. *Anticancer Res.* **9,** 1577–1582
18. Tang, J., Qu, L. K., Zhang, J., Wang, W., Michaelson, J. S., Degenhardt, Y. Y., El-Deiry, W. S., and Yang, X. (2006) Critical role for Daxx in regulating Mdm2. *Nat. Cell Biol.* **8,** 855–862
19. Edson, M. A., Nagaraja, A. K., and Matzuk, M. M. (2009) The mammalian ovary from genesis to revelation. *Endocr. Rev.* **30,** 624–712
20. Chauhan, S. C., Vannatta, K., Ebeling, M. C., Vinayek, N., Watanabe, A., Pandey, K. K., Bell, M. C., Koch, M. D., Aburatani, H., Lio, Y., and Jaggi, M. (2009) Expression and functions of transmembrane mucin MUC13 in ovarian cancer. *Cancer Res.* **69,** 765–774
21. Wang, J., Shiels, C., Sasieni, P., Wu, P. J., Islam, S. A., Freemont, P. S., and Sheer, D. (2004) Promyelocytic leukemia nuclear bodies associate with transcriptionally active genomic regions. *J. Cell Biol.* **164,** 515–526
22. Block, G. J., Eskiw, C. H., Dellaire, G., and Bazett-Jones, D. P. (2006) Transcriptional regulation is affected by subnuclear targeting of reporter plasmids to PML nuclear bodies. *Mol. Cell. Biol.* **26,** 8814–8825
23. Bernardi, R., Guernah, I., Jin, D., Grisendi, S., Alimonti, A., Teruya-Feldstein, J., Cordon-Cardo, C., Simon, M. C., Rafii, S., and Pandolfi, P. P. (2006) PML inhibits HIF-1α translation and neoangiogenesis through repression of mTOR. *Nature* **442,** 779–785
24. Huang, Y. S., Chang, C. C., Huang, T. C., Hsieh, Y. L., and Shih, H. M. (2012) Daxx interacts with and modulates the activity of CREB. *Cell Cycle* **11,** 99–108
25. Yang, S., Jeong, J. H., Brown, A. L., Lee, C. H., Pandolfi, P. P., Chung, J. H., and Kim, M. K. (2006) Promyelocytic leukemia activates Chk2 by mediating Chk2 autophosphorylation. *J. Biol. Chem.* **281,** 26645–26654
26. Dellaire, G., Ching, R. W., Ahmed, K., Jalali, F., Tse, K. C., Bristow, R. G., and Bazett-Jones, D. P. (2006) Promyelocytic leukemia nuclear bodies behave as DNA damage sensors whose response to DNA double-strand breaks is regulated by NBS1 and the kinases ATM, Chk2, and ATR. *J. Cell Biol.* **175,** 55–66
27. Bischof, O., Kirsh, O., Pearson, M., Itahana, K., Pelicci, P. G., and Dejean, A. (2002) Deconstructing PML-induced premature senescence. *EMBO J.* **21,** 3358–3369
28. Bernardi, R., Papa, A., and Pandolfi, P. P. (2008) Regulation of apoptosis by PML and the PML-NBs. *Oncogene* **27,** 6299–6312
29. Joe, Y., Jeong, J. H., Yang, S., Kang, H., Motoyama, N., Pandolfi, P. P., Chung, J. H., and Kim, M. K. (2006) ATR, PML, and CHK2 play a role in arsenic trioxide-induced apoptosis. *J. Biol. Chem.* **281,** 28764–28771
30. Chang, C. C., Naik, M. T., Huang, Y. S., Jeng, J. C., Liao, P. H., Kuo, H. Y., Ho, C. C., Hsieh, Y. L., Lin, C. H., Huang, N. J., Naik, N. M., Kung, C. C., Lin, S. Y., Chen, R. H., Chang, K. S., Huang, T. H., and Shih, H. M. (2011) Structural and functional roles of Daxx SIM phosphorylation in SUMO paralog-selective binding and apoptosis modulation. *Mol. Cell* **42,** 62–74
31. Bernardi, R., and Pandolfi, P. P. (2007) Structure, dynamics and functions of promyelocytic leukaemia nuclear bodies. *Nat. Rev. Mol. Cell Biol.* **8,** 1006–1016
32. Dellaire, G., Ching, R. W., Dehghani, H., Ren, Y., and Bazett-Jones, D. P. (2006) The number of PML nuclear bodies increases in early S phase by a fission mechanism. *J. Cell Sci.* **119,** 1026–1033
33. Lin, D. Y., Huang, Y. S., Jeng, J. C., Kuo, H. Y., Chang, C. C., Chao, T. T., Ho, C. C., Chen, Y. C., Lin, T. P., Fang, H. I., Hung, C. C., Suen, C. S., Hwang, M. J., Chang, K. S., Maul, G. G., and Shih, H. M. (2006) Role of SUMO-interacting motif in Daxx SUMO modification, subnuclear localization, and repression of sumoylated transcription factors. *Mol. Cell* **24,** 341–354
34. Lindsay, C. R., Morozov, V. M., and Ishov, A. M. (2008) PML NBs (ND10) and Daxx: from nuclear structure to protein function. *Front. Biosci.* **13,** 7132–7142